A Unified NTN-IoT Simulator for LoRa CSS and LR-FHSS Uplink Communications over LEO Satellites

Khaoula Kacem
MEDIATRON Lab LR11TIC05
Sup'Com, University of Carthage
Tunis, Tunisia
khaoula.kacem@supcom.tn

Nawel Zangar
LIGM–CNRS UMR 8049
University Gustave Eiffel, ESIEE Paris
F-77420 Marne-la-Vallée, France
nawel.zangar@esiee.fr

Soumaya Hamouda
MEDIATRON Lab LR11TIC05
Sup'Com, University of Carthage
Tunis, Tunisia
soumaya.hamouda@supcom.tn

***Abstract*—Non-Terrestrial Networks (NTNs) based on Low Earth Orbit (LEO) satellites are key enablers for future 6G Internet of Things (IoT) connectivity. However, existing LoRaWAN simulators often overlook NTN-specific effects such as dynamic satellite geometry and Doppler shifts, while support for LR-FHSS fragmentation remains limited. This paper presents UniNTN-Sim, a configurable packet-level simulation framework for LoRaWAN uplink over LEO satellites, supporting both LoRa CSS and LR-FHSS within a unified architecture. The framework integrates trajectory-aware geometry, channel and link-budget modeling, Doppler-aware reception, waveform-specific collision modeling, and packet-level dataset generation. The simulator is evaluated using analytical reference models, an LR-FHSS-Sim-based packet-level check, Doppler and link-budget consistency checks, and a full-channel performance evaluation. The analytical cross-check shows close agreement with the analytical models, with a maximum MAE of 1.2×10^{-3} across all configurations, while the LR-FHSS-Sim-based packet-level check reproduces the expected collision-limited behavior of dense LR-FHSS access. Full-channel results, averaged over 30 independent runs, show that LR-FHSS maintains a high packet-success probability under high device densities, while LoRa CSS experiences a rapid degradation with load. Based on these results, UniNTN-Sim has the potential to serve as a reproducible baseline for future NTN-IoT studies.**

***Index Terms*—NTN-IoT; LEO Satellite; LoRaWAN; LoRa CSS; LR-FHSS; Doppler; Simulator**

I. Introduction

LEO-based Non-Terrestrial Networks (NTNs) are emerging as key enablers of 6G IoT, providing wide-area connectivity for deployments in remote and underserved regions. In this context, LoRaWAN is an attractive candidate because of its low power consumption, long communication range, and suitability for large-scale machine-type communications. However, direct-to-satellite LoRaWAN links are affected by time-varying slant range, elevation-dependent channel conditions, radial velocity, Doppler effects, and finite satellite visibility windows. In dense IoT scenarios, these effects are combined with random-access contention and packet collisions.

The impact of collisions depends strongly on the physical layer. LoRaWAN supports the conventional LoRa Chirp Spread Spectrum (LoRa CSS) and the more recent Long-Range Frequency-Hopping Spread Spectrum (LR-FHSS). In UniNTN-Sim, LoRa CSS reception is resolved at packet level, whereas LR-FHSS relies on replicated headers and payload fragmentation over narrow frequency hops. Consequently, the two waveforms react differently to interference and load, making a fair comparison difficult without a common packet-level framework.

Existing simulators such as LoRaSim [1], FLoRa [2], and ns-3 [3] mainly target terrestrial deployments and do not model LEO satellite geometry and Doppler together with LR-FHSS operation. NTN-oriented tools such as FLoRaSat [4] focus on satellite LoRa/LoRaWAN scenarios, whereas LR-FHSS-Sim [5] is dedicated to LR-FHSS. Analytical studies [6]–[11] investigate Doppler effects, receiver behavior, and capacity, but rely on different assumptions and do not provide a unified packet-level comparison of LoRa CSS and LR-FHSS under identical NTN conditions.

To address this gap, this paper proposes **UniNTN-Sim**, whose main contributions are:

- *Unified LoRa CSS and LR-FHSS framework* under identical LEO geometry, propagation, traffic, and link-budget conditions.
- *Trajectory-aware geometry* computing per-packet elevation, azimuth, slant range, and signed radial velocity, together with the Doppler shift and Doppler-rate quantities used in the reception model.
- *Packet-level collision and capture modeling* adapted to each waveform's structure, namely packet-level reception for LoRa CSS and header-replica/fragment-level reception for LR-FHSS.
- *Analytical, packet-level, Doppler, and link-budget consistency checks* against reference models, an LR-FHSS-Sim-based packet-level baseline, LEO Doppler operating ranges, and elevation-dependent SNR behavior.
- *Packet-level dataset generation* for reproducible analysis and future data-driven adaptation.

The present evaluation uses a single visible LEO satellite pass as a controlled baseline to isolate geometry, propagation,

979-8-3195-0167-7/26/$31.00 ©2026 IEEE

Doppler, and contention effects. Constellation-level effects such as satellite handover and satellite diversity are outside the evaluated scope and are considered future extensions of UniNTN-Sim. The remainder of this paper is organized as follows. Section II reviews related work, Section III presents UniNTN-Sim, Section IV reports the evaluation, and Section V concludes the paper.

II. Related Work

LoRaWAN-based NTN-IoT has been investigated from several complementary perspectives, including analytical LR-FHSS performance evaluation, Doppler impact analysis, receiver design, connectivity analysis, and packet-level simulation. Analytical works on LR-FHSS show how frequency hopping, header replication, and payload fragmentation affect reliability and scalability under different traffic and decoding assumptions [6], [7]. Other studies investigate contention-resolution mechanisms [8], Doppler limitations for LoRa direct-to-satellite links [9], enhanced LR-FHSS receiver design [10], and NTN connectivity analysis [11].

Several simulation tools have also been proposed for LoRaWAN networks. LoRaSim [1], FLoRa [2], and the ns-3 LoRaWAN module [3] mainly address terrestrial deployments. Satellite-oriented tools such as FLoRaSat [4] and FLoRaSat 2 [12] extend LoRaWAN simulation to LEO scenarios, whereas LR-FHSS-Sim [5] focuses on LR-FHSS packet-level performance. Table I summarizes the positioning of these representative simulators.

TABLE I
Positioning of representative LoRaWAN/NTN simulators.

Tool	Scope	LoRa CSS	LR-FHSS
LoRaSim / FLoRa [1], [2]	Terrestrial	Yes	No
FLoRaSat [4]	LEO	Yes	No
FLoRaSat 2 [12]	LEO constellation	Yes	No
LR-FHSS-Sim [5]	LR-FHSS network	No	Yes
UniNTN-Sim	**Controlled LEO pass**	**Yes**	**Yes**

UniNTN-Sim addresses the complementary need for a configurable packet-level framework supporting both LoRa CSS and LR-FHSS uplinks over LEO satellites. It combines satellite geometry, elevation-dependent propagation, Doppler-aware reception, waveform-specific collision and capture mechanisms, and packet-level dataset generation under common simulation assumptions. The objective is to enable controlled CSS/LR-FHSS comparisons and reproducible NTN-IoT studies rather than to replace waveform-specific or constellation-oriented simulators.

III. UniNTN-Sim Architecture and Modeling

A. Overall Framework

UniNTN-Sim is a modular, configuration-driven packet-level simulator. A common configuration fixes the orbital, propagation, traffic, and waveform parameters so that LoRa CSS and LR-FHSS are evaluated under identical external conditions. The present study considers a single visible LEO satellite pass as a controlled setting for isolating geometry, propagation, Doppler, collision, and decoding effects.

As shown in Fig. 1, packet arrivals traverse a common processing chain composed of trajectory-aware geometry, channel and Doppler, and link-budget modules. Reception is then resolved by waveform-specific branches: LoRa CSS uses packet-level SNR, Doppler, collision, and capture checks, whereas LR-FHSS evaluates replicated headers and payload fragments over frequency hops. UniNTN-Sim finally exports network metrics and per-packet records for reproducible analysis.

B. Trajectory-Aware Geometry

For every packet, the geometry module returns elevation $E(t)$, azimuth $A(t)$, slant range $d(t)$, and signed radial velocity $v_r(t) = \dot{d}(t)$. Assuming a spherical Earth of radius R_E and satellite altitude H, the slant range follows [7]

$$d(t) = R_E \left[\sqrt{\left(\frac{R_E + H}{R_E}\right)^2 - \cos^2 E(t)} - \sin E(t) \right]. \quad (1)$$

Positive $v_r(t)$ corresponds to the receding phase and negative $v_r(t)$ to the approaching phase. This signed range rate directly drives the Doppler model.

C. Propagation and Channel Modeling

The channel combines free-space attenuation, environment-dependent clutter loss, log-normal shadowing, and elevation-dependent Rician fading. The free-space path loss is

$$L_{\mathrm{FS}}(t) = 20 \log_{10} d_{\mathrm{km}}(t) + 20 \log_{10} f_{\mathrm{MHz}} + 32.44 \text{ [dB]}. \quad (2)$$

Shadowing follows $X_\sigma \sim \mathcal{N}(0, \sigma^2_{\mathrm{env}})$, while clutter loss L_{cl} is scenario-dependent [13]. The Rician K-factor increases with elevation through linear interpolation between horizon and zenith values [7], [14],

$$K(E) = K_{\min} + \frac{E - E_{\min}}{E_{\max} - E_{\min}} (K_{\max} - K_{\min}), \quad (3)$$

with the complex fading gain normalized such that $\mathbb{E}[|g|^2] = 1$. The received power is

$$P_r = P_t + G_t + G_r - L_{\mathrm{FS}} - L_{\mathrm{cl}} + X_\sigma + 10 \log_{10} |g|^2,$$

and $\mathrm{SNR} = P_r - P_N$, where $P_N = -174 + 10 \log_{10} B + NF$ dBm, with B denoting the receiver bandwidth.

D. Doppler Modeling

The instantaneous Doppler shift and Doppler rate are obtained from the signed radial velocity:

$$f_D(t) = -\frac{v_r(t)}{c} f_c, \qquad \dot{f}_D(t) = \frac{df_D(t)}{dt}. \quad (4)$$

For LoRa CSS, UniNTN-Sim checks the static tolerance $F_{\mathrm{static}} = B/4$ and the dynamic tolerance [9]

$$F_{\mathrm{dyn}} = \frac{L_D B}{3 \cdot 2^{SF}}, \quad (5)$$

against the Doppler excursion accumulated during the packet time-on-air, where $L_D = 16$ when Low Data Rate Optimization is enabled and $L_D = 1$ otherwise.

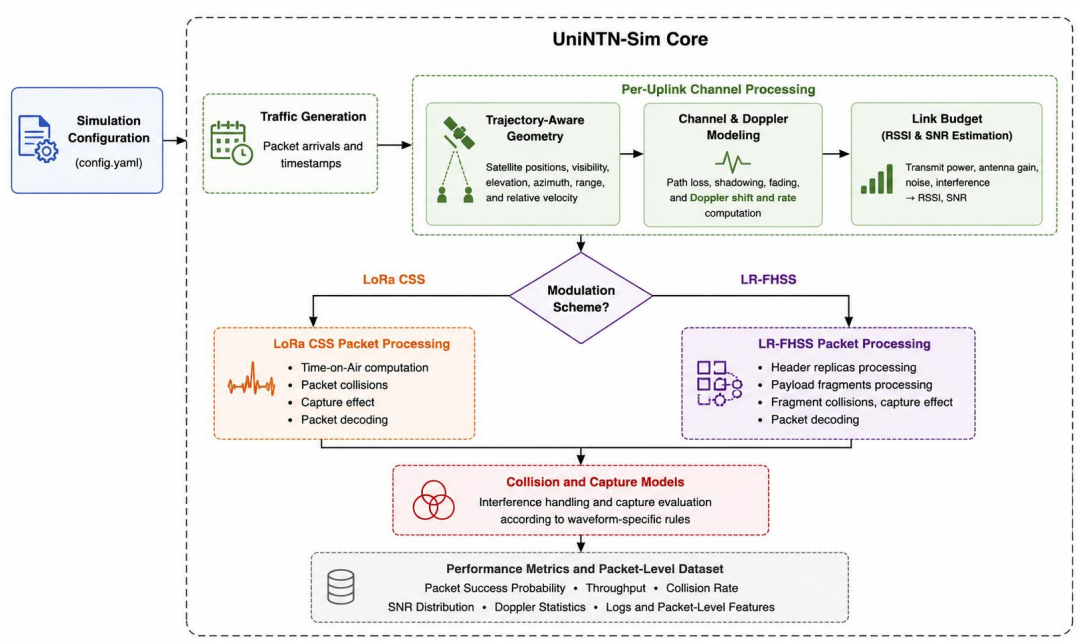


Fig. 1. Overall architecture of the UniNTN-Sim framework.

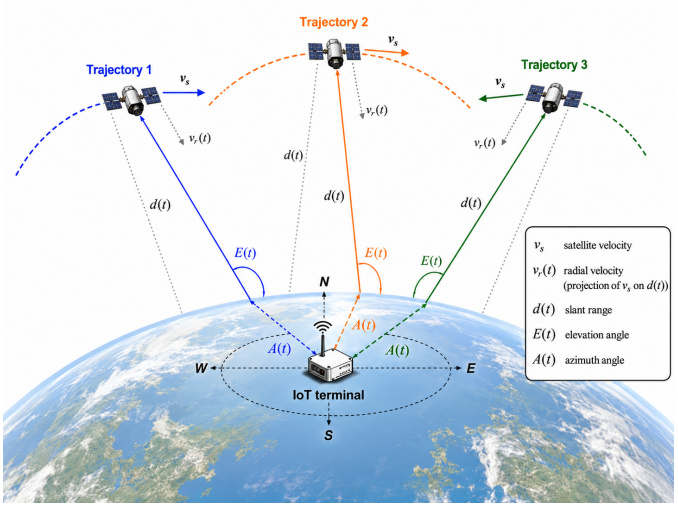


Fig. 2. Trajectory-aware geometry used in UniNTN-Sim. Similar elevation profiles can produce different signed radial velocities because of different line-of-sight projections.

For LR-FHSS, the model uses a static Doppler threshold of 31.65 kHz and an SNR penalty increasing from 0 to 1.5 dB as $|\dot{f}_D|$ increases from 100 to 300 Hz/s [10]. The penalty is applied before header- and fragment-level decoding.

E. Packet Structure and Reception Modeling

For LoRa CSS, time-on-air follows the LoRaWAN model [15]. A packet succeeds when the SF-dependent SNR threshold, Doppler-admissibility conditions, and collision/capture conditions are jointly satisfied. The co-SF capture margin is 6 dB, with inter-SF rejection applied according to SF separation [11], [16].

For LR-FHSS, a frame contains N_h header replicas and $N_f = \lceil (L+2)/M \rceil$ payload fragments, where the two additional bytes account for the CRC and M is the number of bytes per fragment. Each header and fragment is evaluated according to its effective SNR and per-hop interference. A header or fragment is decodable when its effective SNR satisfies $\mathrm{SNR}_{\mathrm{eff}} \geq \Gamma_{\mathrm{LR}} = -13$ dB and the per-hop capture condition holds [7]. A packet is recovered when at least one header and a coding-rate-dependent quorum $\eta = \lceil C R N_f \rceil$ of fragments are decoded [7]:

$$\mathcal{I}_{\mathrm{LR}} = \mathbf{1}_{\{H_{\mathrm{rx}} \geq 1\}} \mathbf{1}_{\{F_{\mathrm{rx}} \geq \eta\}}. \tag{6}$$

This preserves the different collision behavior of LoRa CSS and LR-FHSS rather than applying a common packet-loss rule.

F. Packet-Level Dataset Generation

For each transmission, UniNTN-Sim logs elevation, slant range, radial velocity, Doppler shift and rate, RSSI/SNR, waveform and mode, time-on-air, collision/capture indicators, device count, and the binary reception outcome. These records support reproducible post-processing and future adaptive mode-selection studies.

G. Simulation Parameters

Table II summarizes the main parameters used in the full-channel experiments. The global simulation horizon is 3600 s, whereas reception outcomes are evaluated during the 600 s visible satellite pass. Each operating point is averaged over 30 independent Monte-Carlo replications.

TABLE II
MAIN PARAMETERS USED IN THE FULL-CHANNEL EVALUATION.

Parameter	Value
Simulation / visible pass	3600 s / 600 s
Carrier / altitude	868 MHz / 500 km
Trajectory realizations	50
Payload / devices	10 B / 10^4–2×10^5
Traffic	One uplink report/device/pass
Replications	30 independent runs
Tx power / gains / NF	14 dBm / 2.15, 22.6 dBi / 6 dB
LoRa CSS	125 kHz, CR 4/5, SF7–SF12
LoRa channels / capture	8 / 6 dB
LR-FHSS modes	DR8, DR9; 137 kHz; 280 hopping channels
LR-FHSS SNR threshold	-13 dB

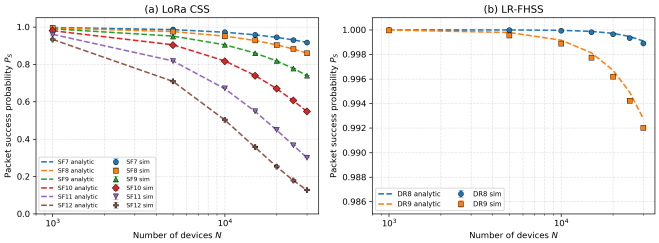


Fig. 3. Analytical cross-check under matched assumptions: (a) LoRa CSS and (b) LR-FHSS packet-success probability. Markers show simulation means with 95% confidence intervals; dashed curves show analytical references.

IV. PERFORMANCE EVALUATION

The goal of this section is to assess the consistency and usefulness of UniNTN-Sim as a simulation baseline. Five complementary checks progressively exercise its main building blocks: an analytical cross-check, an LR-FHSS-Sim-based packet-level cross-check, Doppler and link-budget consistency checks, and a final experiment under the complete simulated NTN channel. Unless otherwise stated, simulation-based operating points are averaged over 30 independent Monte-Carlo replications, with 95% confidence intervals.

A. Analytical Cross-Check

Under simplified and matched assumptions, fading, shadowing, clutter loss, Doppler effects, and capture are disabled so that packet losses are mainly governed by traffic, collisions, and packet-decoding rules. For LoRa CSS, the reference success probability follows the pure-ALOHA model $P_S = \exp(-2G)$. For LR-FHSS, the analytical reference separates header-replica reception from payload-fragment reception and evaluates the probability of receiving at least one header and the required fragment quorum [6], [7].

Fig. 3 shows close agreement for both waveform families. LoRa CSS follows the expected ALOHA degradation as the number of devices increases, with larger spreading factors degrading faster because of their longer time-on-air. LR-FHSS DR8 and DR9 remain close to their analytical references over the considered validation range. Across all configurations, the mean absolute error (MAE) does not exceed 1.2×10^{-3}, while the maximum absolute error does not exceed 2.55×10^{-3}, supporting the consistency of the implemented traffic, collision, fragmentation, and packet-decoding mechanisms under matched assumptions.

TABLE III
ANALYTICAL CROSS-CHECK ERRORS.

Mode	MAE	RMSE	Max. err.
LR-FHSS DR8	7.0×10^{-5}	9.0×10^{-5}	1.9×10^{-4}
LR-FHSS DR9	4.0×10^{-4}	4.7×10^{-4}	7.3×10^{-4}
LoRa SF7	4.8×10^{-4}	6.0×10^{-4}	1.23×10^{-3}
LoRa SF8	5.5×10^{-4}	6.2×10^{-4}	9.2×10^{-4}
LoRa SF9	4.3×10^{-4}	5.9×10^{-4}	1.32×10^{-3}
LoRa SF10	9.0×10^{-4}	1.08×10^{-3}	1.93×10^{-3}
LoRa SF11	1.20×10^{-3}	1.45×10^{-3}	2.42×10^{-3}
LoRa SF12	7.8×10^{-4}	1.10×10^{-3}	2.55×10^{-3}

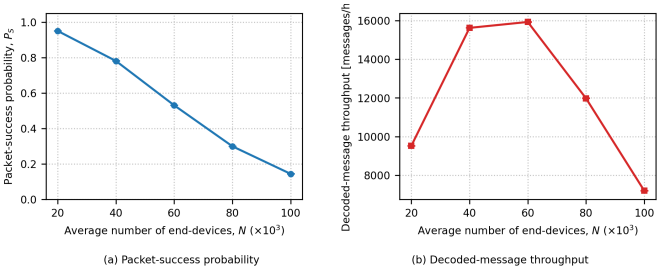


Fig. 4. LR-FHSS-Sim-based packet-level consistency check: (a) packet-success probability and (b) decoded-message throughput.

B. LR-FHSS-Sim-Based Packet-Level Cross-Check

A second consistency check isolates the LR-FHSS packet-processing branch under the simplified collision-limited LR-FHSS-Sim setup [5]. The configuration uses DR8, 20-byte payloads, a 24 h simulation duration, an average inter-arrival time of $T = 900$ s per device, and one grid of 35 occupied-bandwidth channels. The reported number of devices is scaled by a factor of eight to represent the eight available EU LR-FHSS grids. Doppler, fading, shadowing, clutter loss, capture, and link-budget outage are disabled.

As shown in Fig. 4, packet-success probability decreases with device count, whereas decoded-message throughput first increases, reaches a maximum around 6×10^4 devices, and then decreases when packet losses become dominant. This trend-level agreement checks the LR-FHSS traffic generation, header/fragment collision, and quorum-decoding logic. It is not intended as validation of the complete NTN channel.

C. Doppler Cross-Check

For the 868 MHz, 500 km LEO configuration, the simulated Doppler shift remains within ± 21.97 kHz, below the LoRa static tolerance of 31.25 kHz and the LR-FHSS threshold of 31.65 kHz. The mean absolute Doppler rate is 80.38 Hz/s, with a peak magnitude of 335.86 Hz/s near culmination. These values are consistent with the operating ranges reported for LEO direct-to-satellite links [9], [10].

D. Link-Budget Consistency Check

For both waveforms, the simulated SNR increases with elevation as the slant range and free-space loss decrease. For LoRa CSS, the median SNR rises from about -10.7 dB at

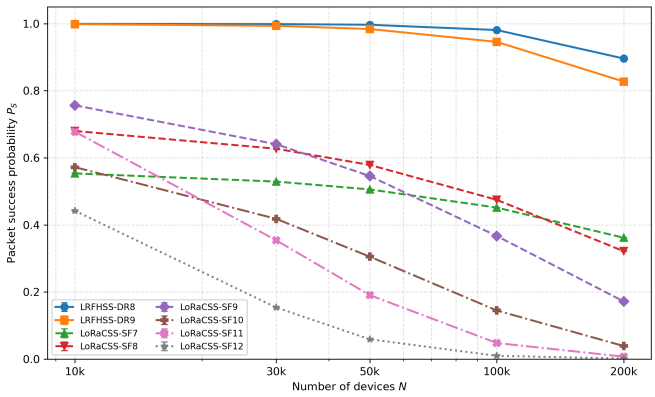


Fig. 5. Packet-success probability versus device count under the complete simulated NTN channel. Points denote means over 30 replications; error bars denote 95% confidence intervals.

low elevation to about 0.5 dB near culmination. For LR-FHSS, the median SNR remains above the $\Gamma_{\mathrm{LR}} = -13$ dB reception threshold under the considered configuration. Consequently, LR-FHSS losses are mainly driven by fragmentation, collisions, and Doppler-rate effects rather than link-budget outage. This check assesses physical consistency and does not constitute validation against satellite measurements.

E. Performance under the Complete Simulated NTN Channel

The final experiment activates the complete simulated channel, including elevation-dependent free-space loss, clutter loss, log-normal shadowing, Rician fading, Doppler shift/rate, and waveform-specific collision and capture mechanisms. The number of contending devices is swept from 10^4 to 2×10^5.

Fig. 5 shows that LR-FHSS achieves higher reliability than LoRa CSS over the considered load range. At $N = 10^5$, DR8 and DR9 reach $P_S = 0.981$ and 0.946; at $N = 2 \times 10^5$, they reach 0.896 and 0.827, respectively. LoRa CSS degrades more sharply: at $N = 2 \times 10^5$, P_S decreases from 0.362 for SF7 to 0.0018 for SF12. Larger spreading factors suffer from longer time-on-air and therefore greater collision exposure.

At lower load, SF9 is the most favorable LoRa spreading factor in the evaluated configuration, whereas SF7 becomes more robust under extreme contention because of its shorter time-on-air. LR-FHSS remains more robust because element-level collisions do not necessarily cause complete packet loss: successful recovery requires at least one header replica and a sufficient number of payload fragments. DR8 remains more robust than DR9 at high load because of its stronger redundancy. These results are specific to the considered 10-byte payload, 500 km altitude, traffic model, and controlled single-satellite pass. Multi-satellite operation, broader sensitivity and scalability analysis, measurement-based validation, and adaptive waveform selection remain future work.

V. Conclusion

This paper presented UniNTN-Sim, a configurable packet-level simulator for LoRaWAN NTN uplinks supporting LoRa CSS and LR-FHSS under common LEO conditions. Analytical and packet-level cross-checks, together with Doppler and link-budget checks, support model consistency. Under the complete simulated NTN channel, LR-FHSS achieved higher packet-success probability than LoRa CSS at high device densities. Future work will consider multi-satellite operation, broader sensitivity and scalability analysis, measurement-based validation, and adaptive waveform selection.

References

[1] M. Bor, U. Roedig, T. Voigt, and J. M. Alonso, "Do LoRa low-power wide-area networks scale?" in *Proceedings of the 19th ACM International Conference on Modeling, Analysis and Simulation of Wireless and Mobile Systems (MSWiM)*, 2016, pp. 59–67.

[2] M. Slabicki, G. Premsankar, and M. Di Francesco, "Adaptive configuration of LoRa networks for dense IoT deployments," in *2018 IEEE/IFIP Network Operations and Management Symposium (NOMS)*, 2018, pp. 1–9.

[3] D. Magrin, M. Centenaro, and L. Vangelista, "Performance evaluation of LoRa networks in a smart city scenario," in *2017 IEEE International Conference on Communications (ICC)*, 2017, pp. 1–7.

[4] J. A. Fraire, P. G. Madoery, M. Ait Mesbah, O. Iova, and F. Valois, "Simulating LoRa-based direct-to-satellite IoT networks with FLoRaSat," in *2022 IEEE 23rd International Symposium on a World of Wireless, Mobile and Multimedia Networks (WoWMoM)*, 2022, pp. 464–470.

[5] J. M. de Souza Sant'Ana, A. Hoeller, H. Alves, and R. D. Souza, "LR-FHSS-Sim: A discrete-event simulator for LR-FHSS networks," in *2024 Joint European Conference on Networks and Communications and 6G Summit (EuCNC/6G Summit)*, 2024, pp. 700–705.

[6] G. Boquet, P. Tuset-Peiro, F. Adelantado, T. Watteyne, and X. Vilajosana, "LR-FHSS: Overview and performance analysis," *IEEE Communications Magazine*, vol. 59, no. 3, pp. 30–36, 2021.

[7] M. A. Ullah, K. Mikhaylov, and H. Alves, "Analysis and simulation of LoRaWAN LR-FHSS for direct-to-satellite scenario," *IEEE Wireless Communications Letters*, vol. 11, no. 3, pp. 548–552, 2022.

[8] J. M. d. S. Sant'Ana, O. Silva Neto, A. Hoeller Jr., J. L. Rebelatto, R. D. Souza, and H. Alves, "Asynchronous contention resolution-aided ALOHA in LR-FHSS networks," *IEEE Internet of Things Journal*, vol. 11, no. 9, pp. 16 684–16 692, 2024.

[9] M. A. Ullah, G. Pasolini, K. Mikhaylov, and H. Alves, "Understanding the limits of LoRa direct-to-satellite: The doppler perspectives," *IEEE Open Journal of the Communications Society*, vol. 5, pp. 51–63, 2024.

[10] D. Maldonado, L. S. Cardoso, J. A. Fraire, A. Guitton, O. Iova, M. Kaneko, and H. Rivano, "Enhanced LR-FHSS receiver for headerless frame recovery in space–terrestrial integrated IoT networks," *Computer Networks*, vol. 257, p. 111018, 2025.

[11] K. Lin and M.-S. Alouini, "Connectivity analysis of LoRaWAN-based nonterrestrial networks for subterranean mMTC," *IEEE Internet of Things Journal*, vol. 12, no. 23, pp. 50 604–50 616, 2025.

[12] A. Y. Choquenaira-Florez, R. Ohs, J. A. Fraire, and H. Rivano, "FLoRaSat 2: Simulating cross-linked direct-to-satellite IoT LEO constellations," in *Proceedings of the 12th Advanced Satellite Multimedia Systems Conference and the 18th Signal Processing for Space Communications Workshop (ASMS/SPSC)*, 2025, pp. 1–8.

[13] 3GPP, "TR 38.811: Study on new radio (nr) to support non-terrestrial networks (release 15)," 3rd Generation Partnership Project (3GPP), Technical Report 38.811, 2020, v15.4.0. [Online]. Available: https://www.3gpp.org

[14] J. Kim, C.-Y. Yang, and J. S. Jang, "Performance analysis of low-earth-orbit (LEO) mobile-satellite system using moment-based approximation of degradation factors," *IEEE Transactions on Vehicular Technology*, vol. 55, no. 3, pp. 876–886, 2006.

[15] Semtech Corporation, "Predicting lorawan capacity (tn1300.05)," Semtech, Tech. Rep., 2024, technical Note.

[16] A. Mahmood, E. Sisinni, L. Guntupalli, R. Rondón, S. A. Hassan, and M. Gidlund, "Scalability analysis of a LoRa network under imperfect orthogonality," *IEEE Transactions on Industrial Informatics*, vol. 15, no. 3, pp. 1425–1436, 2019.